Δελτίο της Ελληνικής Γεωλογικής Εταιρίας τομ. XXXX, 2007
Πρακτικά 11ου Διεθνούς Συνεδρίου, Αθήνα, Μάιος 2007

Bulletin of the Geological Society of Greece vol. XXXX, 2007
Proceedings of the 11th International Congress, Athens, May, 2007

STRAIN RATES IN GREECE USING GPS MEASUREMENTS FROM 1994-2000

Rontogianni S.[1], Clarke P.[1], King M.[1], Lavallée D.[1], England P.[2], Parsons B.[2], and Floyd M.[2]

[1] *University of Newcastle, School of Civil Engineering and Geosciences, UK, Sofia.Rontogianni@ncl.ac.uk, Peter.Clarke@newcastle.ac.uk, M.A.King@newcastle.ac.uk, D.A.Lavallee@newcastle.ac.uk.*

[2] *University of Oxford, Department of Earth Sciences, UK, Philip.England@earth.ox.ac.uk Barry.Parsons@earth.ox.ac.uk Michael.Floyd@earth.ox.ac.uk*

Abstract

Fifteen Greek GPS campaigns from 1994–2001 are reprocessed in ITRF2000 using Bernese v4.2 software. The reference frame is navigated by 43 global, long running IGS sites, which are included in the coordinate final solution together with ~280 local sites. A loosely constrained solution is derived. We combine the 221 daily SINEX files in a least squares approach with the TANYA software, producing the coordinate time series and the velocity field in a European Fixed reference frame. Sites around Chalkidiki and Grevena show a residual motion ~10 mm/yr. Sites around Attica, Evvia, SE Peloponnisos, Aegean Islands have a SW residual motion reaching ~40 mm/yr in South Peloponnisos. The Patras area shows a more south-westerly motion with respect to the rest of the sites, moving ~30-35 mm/yr.
Geodetic strain is derived by two methods: by discrete estimation within contiguous polygons, and by fitting a continuous minimum curvature surface to the velocity field.
Key words: *GPS, Greece, Velocity Field, Strain, Seismic Hazard.*

Περίληψη

Επεξεργαστήκαμε δεκαπέντε, GPS Ελληνικές καμπάνιες από το 1994-2001 σε ITRF2000 χρησιμοποιώντας το Bernese v4.2. Το επίπεδο αναφοράς στελεχώνετε από 43 διεθνείς, με μακρά διάρκεια λειτουργίας IGS σταθμούς που περιλαμβάνονται στις τελικές συντεταγμένες μαζί με περίπου 280 τοπικούς σταθμούς. Οι ελάχιστοι δυνατοί περιορισμοί επιβλήθηκαν στις τελικές συντεταγμένες. Συνδιάσαμε 221 ημερίσιους SINEX φακέλους σε μια προσέγγιση ελαχίστων τετραγώνων με το TANYA πρόγραμμα δημιουργώντας τις χρονικές σειρές των συντεταγμένες και το πεδιο ταχυτήτων σε ένα 'Ευρώπη σταθερό' σύστημα αναφοράς. Οι σταθμοί γύρω από την Χαλκιδική και τα Γρεβενά παρουσιάζουν υπολοιπόμενη κίνηση ~10mm/yr. Σταθμόι γύρω από την Αττική, Εβοια, ΝΑ Πελοπόνησο, νησιά του Αιγαίου εμφανίζουν μια ΝΔ υπολοιπόμενη κίνηση που φτάνει ~40mm/yr στην Νότια Πελοπόνησο. Η περιοχή της Πάτρας δέιχνει μια πιο νοτιοδυτική κινηση σε σύγγριση με τις άλλες περιοχές ~30-35mm/yr.

Η γεωδετική παραμόρφωση υπολογίζεται με δύο μεθόδους, αυτή των διακεκριμένων πολυγώνων και με την εφαρμογή μιας συνεχόμενης ελάχιστης καμπυλότητας επιφάνειας στο πεδίο ταχυτήτων.
Λέξεις κλειδιά: *GPS, Ελλάδα, Πεδίο ταχυτήτων, Παραμόρφωση, Σεισμικος κίνδυνος.*

1. Introduction

The Eastern Mediterranean has been identified as an ideal natural laboratory for studying the kinematics and dynamics of plate interactions (Plag *et al.* 1998). It is one of the most tectonically active regions of Earth's surface (McKenzie 1972, McKenzie 1978) as is demonstrated by its seismicity (Ambraseys 2001, Ambraseys and Jackon 1997, Ambraseys and Jackson 1990). The region is on a convergent plate boundary comprising the subduction of the African Plate under the Eurasian plate while the Arabian plate approaches the Eurasian plate in a northwestward motion. That motion leads the Anatolia plate (defined as the region of Turkey between the North and East Anatolian Faults) to be displaced to the west and rotate in a counterclockwise sense relative to Eurasia (Reilinger *et al.* 1997).

The Hellenic area (Fig. 1) has been the subject of several studies that worked either with earthquake fault plane solution data or with geodetic data in an attempt to solve the tectonic puzzle that surrounds this highly deformed area. Deep seismicity under the sea of Crete is related to the subduction of the northward moving (relative to Eurasia) African oceanic lithosphere, whereas shallow seismicity throughout the Aegean Sea and mainland Greece is related to the southwestward (again relative to Eurasia) extension of the Aegean continental lithosphere driven by a combination of gravitational spreading of the Anatolian continental lithosphere from the east and roll-back of the subducting African plate to the south (Le Pichon and Angelier 1979, Papazachos 1990). The seismicity to the north along the coast of former Yugoslavia, Albania aud NW Greece defines the eastern boundary of the 'Adriatic block' which shows intermediate behaviour between that of the European and African plates. The convergence between the Apulian platform and the Hellenides mountains, the Albanides and the Dinarides is a continental type collision. The lithosphere of the Ionian basin is probably oceanic and the convergent motion results in subduction beneath the Hellenic Trench. The transition between the active lithospheric subduction and the continental collision is located around the Ioniau Islands. (Papazachos and Kiratzi 1996)

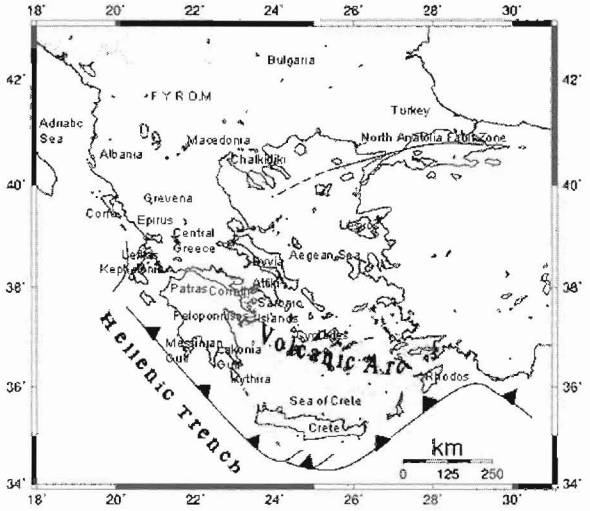

Figure 1-Main features of the Hellenic area and location map

Multiple kinematic (Armijo *et al.* 1996, McKenzie 1970, McKenzie 1978, McKenzie and Jackson 1983, McKenzie and Jackson 1986, Nyst and Thatcher 2004, Taymaz *et al.* 1991, Thatcher 2003) and dynamic models (Goldsworthy *et al.* 2002, Hatzfeld *et al.* 1997, Kreemer *et al.* 2003, Mantovani *et al.* 2000, Meijer aud Wortel 1997) have been proposed as an attempt to describe the observed present-day deformation highlighting many important features of the Hellenic aud surrounding areas (Anatolia, western Turkey) but not developing a single, widely-accepted, cousistent model. Hence the geological questions that still need auswering in the light of the latest data are.

How can the Hellenic area be divided into zones of different deformational style and rate? What amount of geodetic strain is released by seismicity? How important is aseismic deformation?

2. GPS data

The complex tectonics and high deformation rates in the Hellenic area have attracted the curiosity of numerous GPS groups who have organised campaigns and designed networks to assess the strain accumulation throughout this area (Briole *et al.* 2000, Hollenstein *et al.* 2005, Kahle *et al.* 2000, Kahle *et al.* 1999, McClusky *et al.* 2000). This has resulted in a number of overlapping GPS networks. Networks were also designed around Greece in order to strengthen links between sites and fill in areas not previously occupied, in the *HELLENET* and the *SING* projects (Cruddace *et al.* 1999).

Table 1 - GPS campaigns used during the project

Network	Region	Cam-paign/Software	Year	Day of year (DOY)	No. of local sites
Aegean	Aegean	Aegean94,Bernese v4.2	1994	255-272	4
Aegean	Aegean	Aegean96,Bernese v4.2	1996	252-271	4
SING	Argos	Argos98,Bernese v4.2	1998	179-198	48
SING	Patras	Patra98,Bernese v4.2	1998	284-297	28
SING	Chalkidiki, S Peloponnisos	Chasp98,Bernese v4.2	1998	263-275	50
SING	Attiki	Attiki99,Bernese v4.2	1999	276-285	12
SING	Argos, Patras, S Peloponnisos	Paspar99,Bernese v4.2	1999	152-163	54
SING	Chalkidiki	Chalkidiki99,Berne se v4.2	1999	283-295	36
SING	Argos, Patras	Argpa00,Bernese v4.2	2000	184-189	32
SING	Chalkidiki	Chalkidiki00,Berne se v4.2	2000	272-276	30
SING	Corinth	Corinth00,Bernese v4.2	2000	091-195	19
Grevena	Grevena	Grevena96,Bernese v4.2	1996	128-160	41
Grevena	Grevena	Grevena98,Bernese v4.2	1998	153-178	59
Grevena	Grevena	Grevena00,Bernese v4.2	2000	245-254	55
Hellenet	Hellenet	Hellenet97,Bernese v4.2	1997	252-274	72
Egion	Egion	Egion95a,(Jun), GAMIT v10.2	1995	171-176	40
Egion	Egion	Egion95b,(Sep), GAMIT v10.2	1995	276-281	56
Egion	Egion	Egion96,(Jun), GAMIT v10.2	1996	135-153	60
TOTAL					280

Although the majority of these campaign datasets have been analysed and reported previously, it has not been possible to combine them rigorously into a single velocity field because they have been processed using different observation models, constraints, and reference frames. Full variance-covariance information is not always present from previous solutions. Effort made by the researchers to remove the existing constraints was not successful, leading each group to extract its own individual solutions.

Knowing about this drawback we decided to reprocess 18 previous campaigns spanning from 1994-2000 including around 280 local sites (as well as data from the "DION G" GPS pillar in Greece provided by the National Observatory of Athens), combine them and obtain a unified solution for the Greek area (Table 1). We did not work towards removing a co-seismic model from our dataset because the only data from before the 1995 Egion earthquake that we have used are the Aegean campaign (sites ASKT, DION, KATV, XRIS). These are sites distant from the event and so there is no need to remove a co-seismic model.

To produce a better reference frame definition, the frame of each campaign was navigated from as many as 43 IGS and EUREF sites. These sites were chosen to have a global distribution and to have been in continuous operation since 1994 (Fig. 2). The RINEX files for all of these stations were obtained from the Scripps Orbit and Permanent Array Center (SOPAC) http://sopac.ucsd.edu/dataArchive.

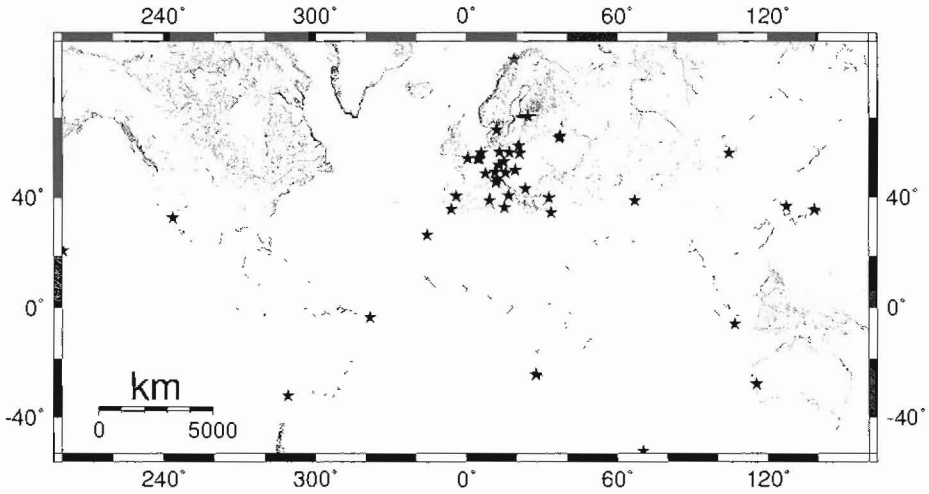

Figure 2 -The 43 Global IGS and EUREF sites used in this project

The raw data were imported in the software via the RINEX (Gurtner 1994) format. Where necessary, transformation from raw (Trimble or Ashtech) format took place using UNAVCO' s TEQC program (Estay and Meertens 1999, UNAVCO). The information given in the RINEX header was corrected in order to agree with the log files. All antenna heights were corrected to agree with the standard ARP (antenna reference point) adopted by IGS. Because the daily networks typically had a mixture of antenna types, we used elevation-dependent phase centre offsets as provided by NOAA (http://www.ngs.noaa.gov/ANTCAL).

3. GPS data processing

For the majority of data processing the Bernese 4.2 GPS software (Beutler *et al.* 2001) was used. As a reference frame for the whole evaluation we used ITRF2000, IGS precise orbits, and we took under consideration the troposphere, ionosphere, and ocean tide loading effects as described in Table 2. We corrected any detected cycle slips, and then attempted to resolve all carrier phase ambiguities to integers as part of each daily network solution, typically with more than 70% success.

The three Egion campaigns were processed in the GAMIT version 10.2 software using a similar strategy but with sessions aligned to the local campaign observations rather than the UT day.

For each campaign, the normal equations of daily sessions were generated and combined into a campaign solution as a check on processing. The daily SINEX files were also produced and saved in order to be used in velocity analysis. For the IGS sites, the a priori velocities were given in ITRF2000 and free network conditions were set up for their coordinates. Table 2 summarises the processing strategy followed.

Table 2 - Processing strategy followed during the project

Session choice	"Day-by-day" strategy, strictly aligned to UT days
Baseline choice	Minimise total baseline length and antenna mismatches, whilst maximising common observation times.
Orbits	IGS precise orbits, held fixed.
Data windowing	10° elevation mask (unless higher in raw data).
Ionosphere model	Ionosphere free observable used; CODE global ionosphere map used to aid ambiguity resolution in wide-lane solutions.
Troposphere model	Saastamoinen model for dry zenith delay; wet zenith delay estimated at 2-hour intervals. Niell mapping function (Niell 1996) (wet and dry).
Tidal loading	IERS 1996 Conventions for solid Earth tides incorporated within Bernese software. Ocean tide loading specified a priori for 11 major constituents using the CSR4.0 ocean tide model, computed using http://www.oso.chalmers.se/~loading/
Ambiguity resolution	Double-difference ambiguities resolved on per-baseline basis within daily network solutions, using either "Quasi Ionosphere Free" model (campaigns Grevena 96, Patras 98, Argos 98) or SIGMA-dependent rounding using a wide-lane followed by ionosphere-free solution (all other campaigns).

4. Velocity field results

Site velocities have been estimated from the combination of 221 loosely constrained daily SINEX files that were created in the Bernese 4.2 processing stage, using the TANYA software (Davies 1997, Davies and Blewitt 2000, Lavallée 2000). Station daily coordinates are rigorously combined using a free network approach (Davies 1997, Davies and Blewitt 2000). In our case the solution coming out from Bernese 4.2 is a loosely constrained solution, and any constraints on the geometry are applied from the fixed IGS orbits. The core_IGS00 SINEX file (the IGS realisation of ITRF2000 Core) was used (Altamimi *et al.* 2002) to navigate the solution to the ITRF2000 reference frame. Antenna height corrections and a three dimensional data-snooping outlier rejection method are also applied if needed at this stage.

The sites were gradually introduced in the solution starting with the ones that had more than 50 observations (the majority of the IGS sites). All sites that were present in more than one campaign and had two or more observations were used in the final solution. An iterative residual outlier rejection boundary of four standard deviations was used to exclude outliers in each station coordinate residual time series. The resulting free network solution is aligned to ITRF2000 by applying 12 Helmert transformations (7 Helmert parameters plus their time derivatives but no scale or scale rate). From the time series of the daily solutions we estimate a kinematic solution which includes a reference epoch position (1999.00) and a constant velocity for each station.

For the sites whose time series were edited, no more than 10% of the overall number of observations were removed. Excluded from the solution are also some of the IGS sites that had very noisy time series The majority of excluded IGS sites are located in the southern hemisphere (i.e. very long baselines, with not enough overlap of visible satellites between the two stations creating the baseline). Excluded sites are YAR1, USUD, SUWN, KOKB, PIN2, KERG, HARK, IRKT. Data for the station ANKR are used until 1999, i.e. before the devastating 1999 Izmit earthquake (17

August M_S 7.4) that took place in this area. No other sites suffered from discernible co-seismic offsets.

The solution in ITRF2000 was expressed in a European Fixed Reference frame by applying the Altamimi *et al.* (2002) absolute Euler pole for Eurasia (Table 3).

Table 3 - Site residuals to the Eurasian absolute Euler pole from Altamimi *et al.* (2002). The IGS and EUREF sites are given in blue

SITE	*Latitude*	*Longitude*	*Residuals North mm/yr*	*Residuals East mm/yr*	*σ-north mm/yr*	*σ-east mm/yr*
AD18	38.324	22.184	-11.942	-18.979	1.150	1.150
AD22	38.356	22.240	-6.494	-25.693	1.330	1.380
AETS	37.244	21.835	-32.503	-25.888	0.360	0.400
AGFA	37.756	24.906	-35.712	-19.086	0.720	0.600
AGMA	38.166	24.065	-25.638	-15.331	0.330	0.300
AGNI	37.669	22.488	-38.244	-14.597	0.520	0.470
AIOL	37.966	24.751	-38.105	-16.042	3.360	5.970
ANKR	39.887	32.758	-2.216	-22.700	0.110	0.100
ARIO	38.327	21.766	-5.400	4.519	0.540	0.600
AS76	38.674	22.441	-9.275	-16.283	1.460	1.460
ASKT	40.928	25.566	-5.345	9.686	0.140	0.130
ASTP	36.586	26.406	-24.371	9.971	0.650	0.670
ATKO	38.494	21.120	-19.418	5.788	0.480	0.410
AY88	39.994	21.743	-11.889	-3.148	0.120	0.120
BORJ	52.277	17.073	0.647	0.609	0.100	0.090
BRUS	50.798	4.359	0.384	-0.947	0.090	0.100
CAGL	39.136	8.973	0.762	-0.315	0.090	0.110
CG05	39.361	23.186	-21.231	-6.483	0.370	0.230
CG19	38.781	22.448	-14.698	-24.597	1.800	1.930
CG20	38.651	22.623	-11.360	-24.721	1.960	2.110
CG22	38.640	22.397	-15.381	-21.988	1.900	1.970
CG30	38.397	22.142	-16.352	-15.099	0.180	0.180
CG31	38.348	22.285	-14.911	-12.221	2.570	2.460
CG32	38.399	22.577	-14.799	-24.606	1.780	1.660
CG33	38.428	22.869	-23.832	-17.744	3.500	3.400
CG42	38.228	21.973	-29.680	-16.217	0.350	0.360
CG43	38.130	22.192	-25.240	-27.161	1.800	1.850
CG47	38.021	22.945	-30.608	-14.920	0.240	0.210
CG48	38.020	23.132	-34.885	-14.303	0.320	0.280
CG49	38.097	23.213	-38.434	-10.379	0.470	0.450
CG50	38.209	23.355	-32.243	-13.348	0.460	0.440
CG52	38.388	23.963	-30.574	-15.069	0.870	0.650
CG53	38.230	23.854	-21.086	-16.692	0.350	0.340
CG54	38.079	23.932	-25.152	-15.588	0.100	0.100
CG55	38.345	24.188	-30.651	-14.906	0.740	0.660

SITE	*Latitude*	*Longitude*	*Residuals North mm/yr*	*Residuals East mm/yr*	*σ-north mm/yr*	*σ-east mm/yr*
CG56	38.086	24.392	-32.612	-19.332	0.330	0.280
CG58	38.018	23.615	-24.079	-22.879	0.410	0.400
CG61	38.014	21.580	-28.914	-21.542	0.450	0.520
CG63	37.723	22.875	-28.101	-17.422	0.440	0.490
CG64	37.795	22.940	-33.097	-17.204	0.810	0.890
CG65	37.804	23.093	-31.207	-17.095	0.300	0.270
CG66	37.822	23.944	-41.672	-20.370	0.610	0.570
CJ00	37.861	22.737	-24.054	-16.810	0.340	0.290
CK00	37.887	22.858	-18.418	-21.010	0.290	0.260
CT00	38.376	22.392	-15.842	-9.211	1.090	1.090
DE30	39.839	21.878	-7.709	-4.753	0.120	0.120
DION	38.079	23.933	-24.780	-17.665	0.100	0.100
DIRO	36.637	22.369	-37.654	-23.137	0.750	0.690
DMNA	37.709	23.068	-31.221	-15.663	0.260	0.230
DREP	38.339	21.849	-13.401	-0.910	0.170	0.190
E000	38.191	22.102	-20.994	-11.634	0.270	0.290
EG56	38.111	22.166	-25.915	-23.509	1.780	1.990
EG62	38.127	22.061	-20.415	-28.997	1.470	1.700
EG75	38.152	22.135	-27.873	-23.109	1.650	1.680
G000	38.066	21.950	-15.614	-19.492	0.250	0.230
G104	40.159	21.359	-3.569	-2.843	0.110	0.110
GOPE	49.914	14.786	-0.031	0.079	0.090	0.090
GR49	40.132	21.290	-3.549	-2.339	0.110	0.110
GR69	40.184	21.498	-3.400	-5.338	0.120	0.110
GRAZ	47.067	15.493	0.940	-0.003	0.090	0.090
H000	38.529	21.980	-8.971	-16.182	0.360	0.330
HERS	50.867	0.336	2.554	9.548	0.090	0.100
HFLK	47.313	11.386	0.896	0.199	0.090	0.090
HIOS	38.443	26.085	-18.437	-17.515	0.570	0.460
I000	38.445	21.903	-10.160	-11.466	0.450	0.340
IERI	40.436	23.848	-3.169	-17.053	0.930	0.720
ILOK	37.442	23.299	-29.485	-18.847	0.220	0.210
IT01	38.342	22.287	-14.843	-15.264	1.320	1.330
IT23	38.407	22.303	-17.568	-21.590	1.420	1.470
IT61	38.492	22.387	-13.000	-28.882	1.350	1.270
JOZE	52.097	21.032	0.207	0.129	0.100	0.090
K000	38.257	21.889	-21.656	-11.187	0.400	0.340
KALI	40.845	22.171	9.265	-0.767	0.650	0.600
KATV	35.952	27.781	-28.183	-12.979	0.370	0.380
KIT3	39.135	66.885	4.418	-7.563	0.140	0.150
KIVE	37.525	22.687	-37.267	-13.647	0.720	0.680
KLKI	41.009	22.833	2.845	-3.887	0.840	0.660
KLTH	36.890	21.803	-42.996	-24.824	0.440	0.390

SITE	*Latitude*	*Longitude*	*Residuals North mm/yr*	*Residuals East mm/yr*	*σ-north mm/yr*	*σ-east mm/yr*
KN03	40.009	21.626	-11.694	-4.391	0.110	0.110
KN29	40.072	21.721	-6.322	-5.159	0.110	0.110
KN43	40.113	21.616	-7.031	-2.725	0.120	0.120
KN49	40.136	21.655	-5.622	-4.683	0.110	0.110
KN88	40.207	21.587	-2.355	-4.156	0.120	0.120
KOIL	37.414	23.114	-27.298	-17.019	0.300	0.260
KOSG	52.178	5.810	1.690	-0.523	0.090	0.090
KOSM	37.087	22.737	-25.950	-15.671	0.320	0.270
KRKR	38.145	23.701	-36.788	-18.951	0.620	0.940
KRNA	39.937	22.544	-12.221	0.591	0.190	0.170
KYLN	37.941	21.136	-8.808	10.075	0.760	0.650
KYRA	36.307	22.984	-19.364	-14.141	0.330	0.270
L000	38.105	21.808	-34.012	-5.656	0.380	0.480
LAGA	40.854	23.540	-3.435	-9.677	0.970	0.730
LAMA	53.892	20.670	0.334	0.472	0.100	0.080
LEON	37.184	22.823	-29.538	-21.048	0.250	0.250
LEPE	38.697	21.291	-6.291	3.414	0.470	0.410
LESV	39.234	26.451	-22.443	-18.486	0.270	0.220
LEVK	38.607	22.197	-14.244	-9.895	0.370	0.340
LGRN	37.677	24.000	-28.621	-13.394	0.570	0.500
LI29	40.063	21.939	-8.787	-4.596	0.120	0.120
LI74	40.210	21.899	-7.709	-3.079	0.120	0.110
LIMN	39.851	25.126	-15.451	-17.129	0.360	0.280
LIPO	39.676	21.846	-9.491	-5.959	0.140	0.130
LO79	40.188	22.043	-7.755	-4.250	0.130	0.150
LTSA	37.955	23.996	-27.806	-18.708	0.810	0.680
MADR	40.429	355.750	0.832	-0.729	0.090	0.120
MAOR	38.186	21.390	-19.260	1.380	0.440	0.360
MAS1	27.764	344.367	2.900	-1.705	0.090	0.150
MATE	40.649	16.704	4.725	-0.318	0.090	0.100
MDVO	56.027	37.224	4.866	2.675	0.110	0.080
MEDI	44.520	11.647	2.394	2.183	0.090	0.100
MESS	38.370	21.122	-11.678	0.873	0.510	0.440
METS	60.217	24.395	-0.877	3.522	0.100	0.080
MLDR	37.750	22.644	-17.967	-8.902	0.740	0.600
MLSS	37.946	21.352	-19.705	-3.540	0.510	0.470
MLVN	37.171	22.252	-32.641	-14.300	0.610	0.680
MNVS	36.743	23.078	-35.182	-18.712	0.420	0.360
MYRT	38.075	21.504	-23.379	-13.383	0.970	0.920
NEVR	41.355	23.846	-4.765	-24.593	0.360	0.280
NICO	35.141	33.396	4.094	-10.654	0.110	0.110
NOTO	36.876	14.990	4.108	-5.258	0.090	0.110
ONSA	57.395	11.926	-0.071	0.319	0.090	0.090

SITE	*Latitude*	*Longitude*	*Residuals North mm/yr*	*Residuals East mm/yr*	*σ-north mm/yr*	*σ-east mm/yr*
OREI	37.347	22.656	-24.290	-13.432	0.540	0.530
OXIA	39.764	21.936	-6.093	-14.067	0.380	0.330
P842	40.601	21.677	-8.492	-4.637	0.160	0.140
PENC	47.790	19.282	0.580	0.395	0.100	0.090
PHEL	37.296	23.172	-32.107	-14.404	0.590	0.540
PIGA	37.065	22.911	-35.862	-13.655	0.530	0.490
PLAT	40.642	23.362	-7.826	-11.609	0.830	0.660
PLNI	37.176	22.129	-21.087	-20.697	0.460	0.430
POTS	52.379	13.066	-0.063	-0.722	0.090	0.090
PRST	36.876	22.243	-35.360	-19.702	0.480	0.460
PSMS	40.373	23.444	-10.691	-28.530	0.160	0.140
PYLO	36.887	21.695	-43.936	-18.827	0.400	0.340
RASK	37.978	23.309	-19.325	-10.248	0.340	0.310
RIOE	38.311	21.780	-9.319	-15.636	0.950	2.190
RION	38.311	21.783	-12.886	-15.373	0.680	0.600
ROML	35.404	24.694	-31.359	-13.604	0.240	0.220
SFER	36.464	353.794	2.120	-1.419	0.090	0.120
SI19	40.305	21.702	-5.743	-4.279	0.120	0.120
SI34	40.343	21.562	-4.349	-1.461	0.120	0.110
SI80	40.473	21.510	-4.504	-2.874	0.110	0.110
SIFB	40.238	21.569	3.712	-5.944	0.180	0.170
SOFI	42.556	23.395	-1.902	-0.787	0.100	0.100
STHN	39.994	23.919	-11.378	-10.284	0.120	0.110
STRF	37.069	21.866	-38.403	-31.661	0.880	1.100
STRV	37.098	22.409	-47.130	-24.686	1.230	0.970
THEO	40.964	23.120	5.852	-12.235	0.880	0.850
THIR	36.346	25.439	-22.615	-9.052	0.390	0.510
THOM	38.392	21.488	-25.462	-18.061	0.720	0.680
TOLO	38.324	22.184	-12.840	-8.414	0.470	0.430
TSUK	40.858	21.881	-4.418	-13.363	0.190	0.170
TZIA	37.623	24.368	-36.845	-19.679	0.590	0.610
UPAD	45.407	11.878	2.841	0.317	0.090	0.100
VELI	36.718	22.948	-39.910	-16.549	0.220	0.200
VILL	40.444	356.048	0.100	2.957	0.090	0.120
VRES	40.798	23.136	0.759	-6.613	0.540	0.410
VRMS	37.464	23.469	-31.022	-22.437	0.600	0.530
WARE	50.690	5.245	1.204	-1.505	0.090	0.100
WTZR	49.144	12.879	0.173	-0.260	0.090	0.090
XRIS	36.791	21.878	-30.109	-18.627	0.120	0.130
YITH	36.776	22.560	-44.271	-9.721	0.590	0.560
ZIMM	46.877	7.465	0.859	-0.414	0.090	0.100
ZWEN	55.699	36.759	-0.086	4.431	0.110	0.080

The sites around the Chalkidiki and Grevena area show, in their majority, a very small residual motion of around 10 mm/yr. Further south there is an obvious SW motion of the sites around Attica, Evvia, east and south Peloponnisos as well as the Aegean Islands. This motion increases from around ~25 mm/yr for the Aegean islands to around 30mm/yr near Attica, Evvia and the eastern Peloponnisos coast, and reaches ~40 mm/yr for the sites in southern Peloponnisos. This increase has also been suggested previously e.g. Cocard *et al.* (1999) and Peter *et al.* (1998). The rapid displacement that is concentrated in the small area of the Corinth and Patras Gulfs is very prominent. The Patras area shows south-westerly motion of ~30-35 mm/yr.

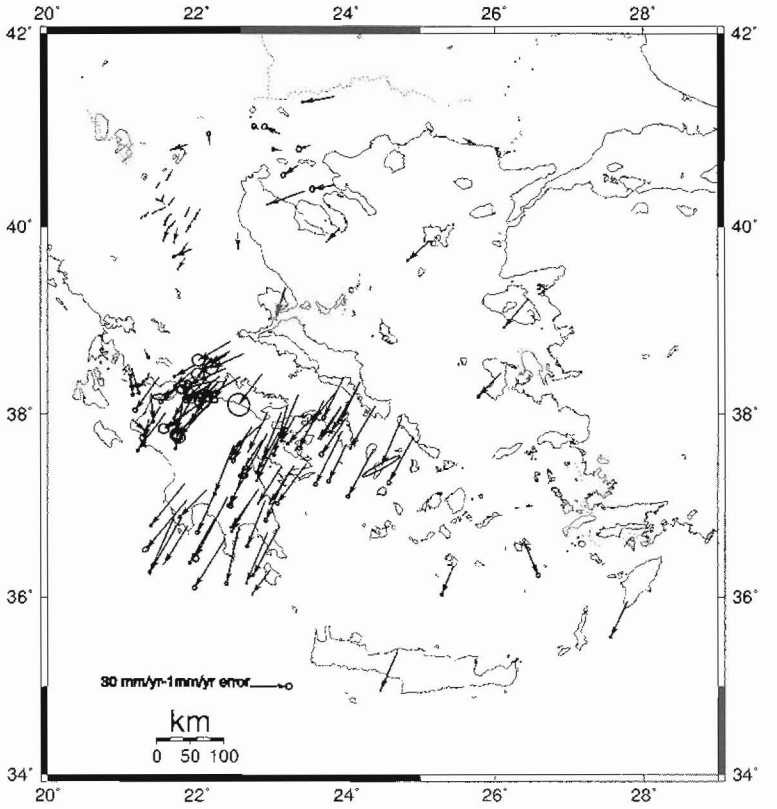

Figure 3 - Velocities for the Greek sites in a Eurasian Fixed reference frame from the period 1994-2000 as formed in this study. 95 % confidence error ellipses are shown

5. Strain analysis

The next step of data analysis is to compute geodetic strain-rate tensors and rotation rates by using two different methods. The first is the polygon method which allows us to define the region where the strain is to be computed (e.g. based on geological criteria). The second method of deriving strain rates calculates the stain by applying a continuous curvature gridding to the horizontal velocity field data, and is independent of geological preferences and allows interpolation between points.

For the first method the area is divided up into polygonal regions bounded by geodetic monuments. The strain rate is assumed to be uniform within each polygonal region and constant with respect with time. No assumptions are made regarding the continuity of velocity or strain rate between regions (Frank 1966, Welsch 1983). The choice of the polygons is very important but somewhat arbitrary although reasonable criteria can be adopted. The Greek area is quite compli-

cated because it contains many active faults, most of which appear to have segments of around 15-20 km in length. Primarily we created the smallest possible polygons according to major tectonic zones as defined by previous researchers (Kahle *et al.* 1998, Le Pichon and Angelier 1979, Le Pichon *et al.* 1995, Papazachos *et al.* 1999). Following this step, neighbouring polygons with similar strain pattern are merged. We tried to ensure that the final polygons bound the whole of either main fault zones or trough zones. That was not always possible because the faults can be quite small or concentrated in a narrow area (e.g. Corinth Gulf, Evvia Gulf). In the final polygons the uniform strain is in a good fit (root mean square weighted residual applied) to all the stations that pertain to it. In total 22 polygons were formed. The principal horizontal strain rates, for each of the chosen 22 polygous, are computed using the program *polystr2* (Clarke 1996). From tbe velocity gradient tensor the strain parameters and their formal errors are derived. Table 4 and Figure 4 summarise the results for each polygou. There is generally a large uncertainty in the azimuth of the principal strain rates, although their magnitudes are relatively certain. Figure 5 presents the geodetic rigid body rotation for each of the 22 polygons. Strong clockwise rotation is observed around the North Eastern Aegean, Gulf of Corinth, and Gulf of Evvia, with smaller rates around the Grevena and Chalkidiki areas. The sense of rotation changes in the South Aegean and Cyclades area where anti-clockwise rotation is present.

Table 4 - Principal horizontal strain rates (ppm/year), azimuth of most compressive principal strain (degrees), and rates of rotation and dilatation (ppm/year)

Polygon	Eps1 (ppm/yr)	1σ	Eps2 (ppm/yr)	1σ	Azim (deg)	1σ	Rotation (deg/Myr)	1σ	Dilatation (ppm/yr)	1σ
1	0 174	0.006	-0.037	0.005	-86 9	1.50	6 6	0.22	0 138	0.008
2	0 108	0.004	0.019	0.005	-75 5	3 61	-0.3	0.17	0.127	0.006
3	0 072	0 008	-0.019	0.006	-68 5	8.40	10.5	0.29	0.054	0.010
4	0 281	0.010	0.057	0.009	-79.1	2 81	-6 7	0.39	0.338	0.013
5	0 092	0.007	-0.179	0.019	86 7	3.44	2.1	0 65	-0.087	0.020
6	0 072	0.002	-0.125	0.004	75.9	1 11	0.6	0.12	-0.053	0.119
7	0.197	0 005	-0.214	0.005	85 7	0.66	2.2	0 19	-0.017	0.007
8	0 261	0.008	-0 013	0.024	78 2	4.53	2.5	0.73	0.248	0.025
9	0.021	0 026	-0 129	0.071	-36.1	50.2 1	11.1	2.16	-0.108	0 076
10	0.113	0.014	0 004	0.009	-4.5	6.20	8.0	0.47	0 117	0.017
11	0.039	0.004	-0.018	0 004	1.5	4.56	1.9	0.18	0.020	0.006
12	0.143	0.007	-0 074	0 005	75.5	2.02	3.2	0.23	0.069	0 008
13	0.023	0.003	-0 045	0 003	50.1	43.9 9	3.6	0.11	-0.022	0.003
14	0.080	0.002	-0.043	0 001	-76.2	1.04	1 2	0.07	0.037	0.003
15	0.095	0.004	0.001	0.002	-64.3	4.87	-2 5	0.13	0.096	0.005
16	0.003	0.002	-0.164	0 008	27.3	5.83	-1.5	0 23	-0.161	0.008
17	0.091	0.004	-0.011	0 001	-45.2	50.7 8	-1 9	0.11	0.079	0.004
18	0.093	0.005	-0.013	0.003	-78.6	2.72	1.6	0.18	0.080	0.005
19	0.135	0.014	-0.449	0.009	0.5	1.15	-2.2	0.47	-0.314	0.016
20	0.069	0.001	-0.052	0.001	62.0	1.84	1.8	0 05	0.017	0.002
21	0.113	0.003	-0.038	0 001	82 6	0.80	-1.4	0.07	0.075	0.003
22	0.166	0.002	-0.008	0.001	-42.9	48.7 0	6.3	0.07	0.174	0.003

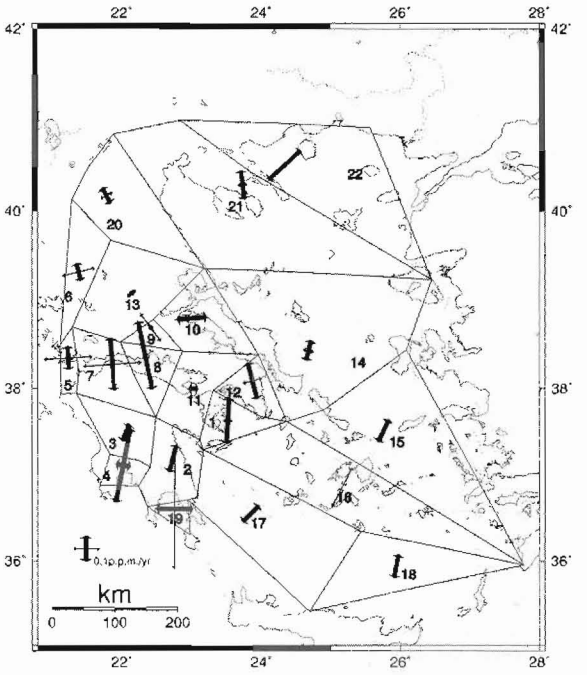

Figure 4 - Principal strain rates computed for the 22 polygonal regions. Extensional axes are shown as thick lines and compressional axes as shown as thin lines. Results are given in ppm/yr

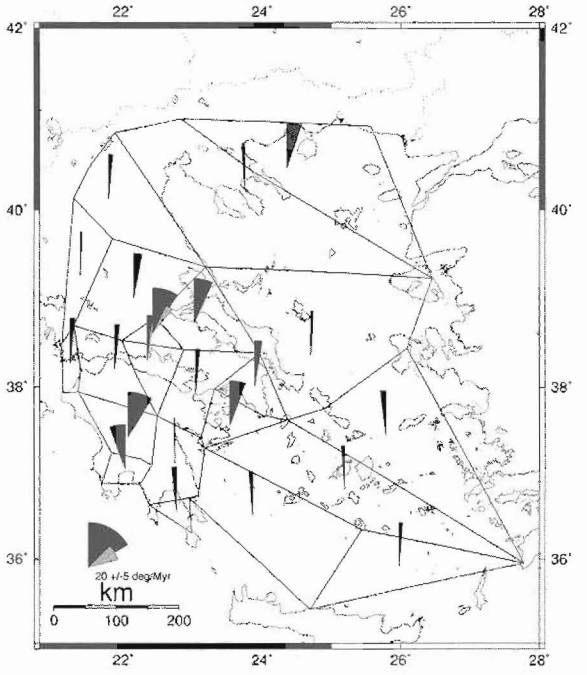

Figure 5 - Geodetic rigid-body rotation rates compnted from the polygonal regions (deg/Myr). Uncertainties (95 % confidence) are shown in grey

The second method of deriving horizontal geodetic strain rates is independent of geological preferences, depending only on the velocity field data. We applied a continuous curvature gridding to the horizontal velocity field data allowing interpolation between points. Three different grid spacing values were tested (10, 30, 40 minutes) with the 30 minute grid spacing chosen. The 10 minute grid did not show any regions of different strain patterns when compared with the 30 minute grid, whereas the 40 minute grid masked detail that was observed with the 30 minute grid. The principal strain rates from the above are shown in Figure 6.

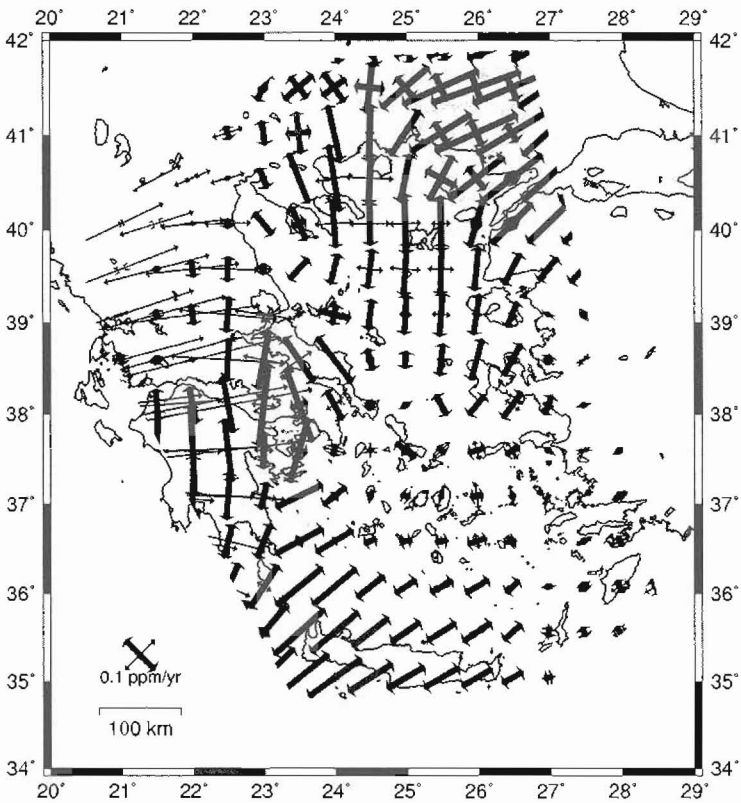

Figure 6 - Principal strain rates computed from the minimum curvature grid method

There is a very good agreement when comparing strain rates between the grid and polygon methods. In general the Hellenic area experiences a rapid extensional deformation. This model shows areas bounded by fault systems e.g. Gulf of Evvia, Gulf of Corinth, and Gulf of Messinia undergoing rapid extension. The central and southern Aegean are extending. The region around the Cyclades is almost strain free. In western Greece where continental collision takes places, rapid compression is present increasing in the Gulf of Patras. Differences are observed near to the edges of the grid (e.g. Laconia Gulf and western Greece) where there are too few data points for the interpolation method to be reliable and spurious effects occur. Agreement is observed in north Greece (Grevena area), north Aegean, Corinth Gulf area, Patras Gulf area, western Peloponnisos, south Aegean (Sea of Crete). An obvious difference is observed around the northern Gulf of Evvia. In the polygon method (polygon 10, Fig. 4) the direction of deformation is E-W, whereas in the gridding methods the direction of deformation is NNW-SSE. However, in the polygon method the azimuth has a large uncertainty because only five relatively closely-spaced data points are used, whereas in the gridding methods data from the wider region will have an influence. In both methods the deformation is extension at ~0.11 ppm/yr. The geodetic-rigid body rotation rates show a

similar pattern for all the methods applied. Strong clockwise rotation is observed in the Peloponnisos area, Central Greece and north Aegean Sea, while rapid counter-clockwise rotation is observed in the central Aegean, Cyclades and Sea of Crete.

6. Conclusion

GPS measurements from 1994 -2000 were reprocessed in order to determine the magnitude and style of deformation throughout the Hellenic region, in a Europe-fixed reference frame. Results from previous studies cannot be rigorously combined because the reference frame constraints and the conventions of the processing software used cannot be removed using the available information. 18 GPS campaigns from 1994 –2001 covering ~280 local sites have been included, with a reference frame navigated by 43 global, long-running IGS sites. Using the Altamimi *et al.* (2002) European absolute Euler pole, a solution is derived in a Europe-fixed reference frame. In the Hellenic region, sites around the Chalkidiki and Grevena areas show a small residual motion of around 10 mm/yr with respect to stable Europe. Sites around Attica, Evvia, and the eastern and southern Peloponnisos, as well as the Aegean Islands, have a SW motion which increases from ~25 mm/yr for the Aegean islands to around 30 mm/yr around Attica, Evvia and the eastern Peloponnisos coast and ~40 mm/yr for sites in the southern Peloponnisos. The Patras area shows a residual motion of around 30-35mm/yr.

Geodetic strain-rate tensors and rotation rates are computed firstly within independent contiguous polygons, and secondly by applying continuous curvature gridding to the horizontal velocity field data. The two methods give very similar results. In general terms the Hellenic area is a region undergoing a rapid extensional deformation. Areas bounded by fault systems e.g. Gulf of Evvia, Gulf of Corinth, and Gulf of Messinia undergo strong extension. The central and south Aegean are also extending but the Cyclades area is almost strain free. In western Greece where continental collision takes place, strong compression is present, increasing in Gulf of Patras. Clockwise rotation is observed in Central Greece around the Gulfs of Corinth and Evvia, turning to anticlockwise rotation in the south Aegean and South Peloponnisos.

7. References

Altamimi, Z., Sillard, P., and Boucher, C., 2002. ITRF2000: A new release of the International Terrestrial Reference Frame for earth science applications, *J.Geophys.Res*, 107(B10), 2214. doi:10.1029/2001JB000561

Ambraseys, N., 2001. Reassessment of earthquakes,1900-1999, in the Eastern Mediterranean and the Middle East, *Geophys.J.Int*, 145, 471-485.

Ambraseys, N., and Jackon, J., 1997. Seismicity and strain in the Gulf of Corinth (Greece) since 1694, *J.Earthq. Eng*, 1(3), 433-474.

Ambraseys, N., and Jackson, J., 1990. Seismicity and associated strain of central Greece between 1890 and 1988, *Geophys.J.Int*, 101, 663-708.

Armijo, R., Meyer, B., King, G.C.P., Rigo, A., and Papanastasiou, D., 1996. Quaternary evolution of the Corinth Rift and its implications for the Late Cenozoic evolution of the Aegean, *Geophys.J.Int*, 126, 11-53.

Beutler, G., et al., 2001. *Bernese GPS software Version 4.2*, Astronomical Institute, University of Berne 2001.

Briole, P., et al., 2000. Active deformation of the Corinth rift, Greece: Results from repeated Global Positioning System surveys between 1990 and 1995, *J.Geophys.Res*, 105(B11), 25.605-25.625.

Clarke, P.J., 1996. *Tectonic motion and tectonic deformation in Greece from GPS measurements*, University of Oxford, Exeter College, Oxford.

Cocard, M., et al., 1999. New constraints on the rapid crustal motion of the Aegean region: recent results inferred from GPS measurements (1993-1998) across the West Hellenic Arc, Greece, *Earth Planet.Sci.Lett*, 172, 39-47.

Cruddace, P.R., et al., 1999. An interdisciplinary approach to studying seismic hazard throughout Greece. In Geodesy beyond 2000: the challenges of the first decate, *International Association of Geodesy Symposia,* 121, 279-284.

Davies, P., 1997. *Assembling the IGS polyhedron. a densinfied weekly GPS terrestrial reference frame*, University of newcastle Upon Tyne, Newcastle Upon Tyne.

Davies, R.R., and Blewitt, G., 2000. Methodology for global geodetic time series estimation: A new tool for geodynamics, *J.Geophys.Res*, 105(B5), 11.083-11.100.

Estay, L., and Meertens, C., 1999. TEQC: The Multi-Pnrpose Toolkit for GPS/GLONASS data, *GPS solutions*, 3(1): 42-42.

Frank, F.C., 1966. Deduction of earth strains from survey data, *Bull.Seismol.Soc.Am*, 56(1), 32-42.

Goldsworthy, M., Jackson, J., and Hains, A.J., 2002. The continuity of the active fault systems in Greece, *Geophys.J.Int,* 148, 596-618.

Gurtner, W., 1994. RINEX: The Receiver Independent Exchange Format, *GPS WORLD*, 5(7): 48-52.

Hatzfeld, D., Martinod, J., Bastet, G., and Gautier, P., 1997. An analogue experiment for the Aegean to describe the contribution of gravitational potential energy, *J.Geophys.Res*, 102, 649-659.

Hollenstein, C., Geiger, A., Kahle, H.-G., and Veis, G., 2005. CGPS time-series and trajectories of crustal motion along the West Hellenic Arc, *Geophys.J.Int*, 164, 182-191. doi:10.1111/j.1365-246X.2005.02804.x

Kahle, H.-G., et al., 2000. GPS-derived strain rate field within the boundary zones of the Eurasian, African, and Arabian Plates, *J.Geophys.Res*, 105(B10), 23.353-23.370.

Kahle, H.-G., et al., 1999. The GPS strain rate field in the Aegean Sea and western Anatolia, *Geophys.Res.Lett*, 26(16), 2513-2516.

Kahle, H.-G., et al., 1998. The strain rate field in the eastern Mediterranean region estimated by repeated GPS measurements, *Tectonophysics*, 294, 237-252.

Kreemer, C., Holt, W.E., and Hains, A.J., 2003. An integrated global model of present-day plate motions and plate boundary deformation, *Geophys.J.Int*, 154, 8-34.

Lavallée, D.A., 2000. *Tectonic plate motions from global GPS measurements*, University of Newcastle Upon Tyne, Newcastle Upon Tyne.

Le Pichon, X., and Angelier, J., 1979. The Hellenic arc and trench system: a key to the evolution of eastren Medoterranean, *Tectonophysics*, 60, 1-42.

Le Pichon, X., Chamot-Rooke, N., and Lallemant, S., 1995. Geodetic determination of the kinematics of central Greece with respect to Europe: Implications for eastern Mediterranean tectonics, *J.Geophys.Res*, 100(B7), 12.675-12.690.

Mantovani, E., et al., 2000. Role of kinematically induced horizontal forces in Mediterranean tectonics: insight from numerical modelling, *J.Geodyn*, 30, 287-320.

McClusky, S., et al., 2000. Global Positioning System Constraints on plate kinematics and dynamics in the eastren Mediterranean and Caucasus, *J.Geophys.Res*, 105(B3), 5695-5719.

McKenzie, D.P., 1970. Plate Tectonics of the Mediterranean Region, *Nature*, 226, 239-243.

McKenzie, D.P., 1972. Active tectonics of the Mediterranean Region, *Geophys.J.R.astr.Soc*, 30, 109-185.

McKenzie, D.P., 1978. Active tectonics of the Alpine-Himalayan Belt: the Aegean Sea and surrounding regions, *Geophys.J.R.astr.Soc*, 55,: 217-254.

McKenzie, D.P., and Jackson, J., 1983. The relationship between strain rates, crustal thickening, paleomagnetism, finite strain and fault movements within a deforming zone, *Earth Planet.Sci.Lett*, 65, 182-202.

McKenzie, D.P., and Jackson, J., 1986. A block model of distributed deformation by faulting, *J.Geol.Soc.London*, 143, 349-353.

Meijer , P.T., and Wortel, M.J.R., 1997. Present-day dynamics of the Aegean region: a model analysis of the horizontal pattern of stress and deformation, *Tectonics*, 16, 879-895.

Niell, A.E., 1996. Global mapping functions or the atmosphere delay at radio wavelengths, *J.Geophys.Res*, 101(B2), 3227-3246.

Nyst, M.C.J., and Thatcher, W., 2004. New constraints on the active tectonic deformation of the Aegean, *J.Geophys.Res*, 109, B11406. doi:10.1029/2003JB002830

Papazachos, B.C., 1990. Seismicity of the Aegean and the surrounding area, *Tectonophysics*, 178, 287-308

Papazachos, B.C., Papaioannou, C., Papazachos, C.B., and A.S, S., 1999. Rupture zones in the Aegean region, *Tectonophysics*, 308, 205-221.

Papazachos, C.B., and Kiratzi, A., 1996. A detailed study of the active crustal deformation in the Aegean and surrounding area, *Tectonophysics*, 253, 129-153.

Peter, J.D., et al., 1998. Establishment of continuous GPS network across Kephalonia Fault Zone, Ionian islands, Greece, *Tectonophysics*, 294, 253-260.

Plag, H.-P., et al., 1998. Scientific objectives of current and future WEGENER activities, *Tectonophysics*, 294, 177-223.

Reilinger, R., et al., 1997. Global Positioning System measurements of present-day crustal mmovements in the Arabia-Africa-Eurasia plate collision zone, *J.Geophys.Res*, 102(B5), 9983-9999.

SOPAC, Scripps Orbit and Permanent Array Center

http://sopac.ucsd.edu/dataArchive/: (downloaded, May 2006)

Taymaz, T., Jackson, J., and McKenzie, D.P., 1991. Active tctonics of the north and central Aegean Sea, *Geophys.J.Int*, 106, 433-490.

Thatcher, W., 2003. GPS Constraints on the Kinematics of Continental Deformation, *Internat.Geology Review*, 45, 191-212.

UNAVCO, TEQC-tutorial. http://facility.unavco.org/software/teqc/teqc.html: (downloaded, May 2006)

Welsch, W.M., 1983. Finite element analysis of strain patterns from geodetic observations across a plate margin, *Tectonophysics*, 97, 57-71.